

The ℓ_1 - ℓ_2 minimization with rotation for sparse approximation in uncertainty quantification

Mengqi Hu¹, Yifei Lou², and Xiu Yang^{*3}

^{1,2}Department of Mathematical Sciences, University of Texas Dallas, Richardson, TX 75080, USA

³Department of Industrial and Systems Engineering, Lehigh University, PA 18015, USA

Abstract

This paper proposes a combination of rotational compressive sensing with the ℓ_1 - ℓ_2 minimization to estimate coefficients of generalized polynomial chaos (gPC) used in uncertainty quantification. In particular, we aim to identify a rotation matrix such that the gPC of a set of random variables after the rotation has a sparser representation. However, this rotational approach alters the underlying linear system to be solved, which makes finding the sparse coefficients much more difficult than the case without rotation. We further adopt the ℓ_1 - ℓ_2 minimization that is more suited for such ill-posed problems in compressive sensing (CS) than the classic ℓ_1 approach. We conduct extensive experiments on standard gPC problem settings, showing superior performance of the proposed combination of rotation and ℓ_1 - ℓ_2 minimization over the ones without rotation and with rotation but using the ℓ_1 minimization.

Keywords Generalized polynomial chaos, uncertainty quantification, iterative rotations, the ℓ_1 - ℓ_2 minimization

1 Introduction

Surrogate model (also known as “response surface”) plays an important role in uncertainty quantification (UQ), as it can efficiently evaluate the quantity of interest (QoI) of a system given a set of inputs. Specifically, in parametric uncertainty study, the input usually refers to a set of parameters in the system, while the QoI can be observables such as mass, density, pressure, velocity, or even a trajectory of a dynamical system. The uncertainty in the system’s parameters typically originates from the lack of physical knowledge, inaccurate measurements, etc. Therefore, it is common to treat these parameters as random variables, and statistics, e.g., mean, variance, and probability density function (PDF) of the QoI with respect to such random parameters are crucial in understanding the behavior of the system.

A widely used surrogate model in applied mathematics and engineering studies is the generalized polynomial chaos (gPC) expansion [23, 61] which uses orthogonal polynomials associated with measures of the aforementioned random variables. Under some conditions, the gPC expansion converges to the QoI in a Hilbert space as the number of polynomials increases [61, 9, 42, 21]. Similar to the Fourier expansion, the basis functions are given to achieve the task of identifying gPC coefficients. Both *intrusive* methods (e.g., stochastic Galerkin) and *non-intrusive* methods (e.g., probabilistic collocation method) have been developed [23, 61, 55, 60, 4] to compute the gPC coefficients. The latter is specifically more desirable to study a complex system, as it does not require modifying the computational models or simulation codes. In particular, the gPC coefficients can be calculated based on input samples and corresponding output using least squared fitting, probabilistic collocation method, etc [23, 61, 55, 60, 4].

*Corresponding author: xiy518@lehigh.edu

However, in many practical problems, it is prohibitive to obtain a large amount of output samples used in the non-intrusive methods, since it is costly to measure the QoI in experiments or conduct simulations using a complicated model. Consequently, one shall consider an under-determined measurement matrix, denoted as Ψ of size $M \times N$ with $M < N$ (or even $M \ll N$), where M is the size of available output samples and N is the number of basis functions used in the gPC expansion. When the solution to the under-determined system is sparse, compressive sensing (CS) techniques [11, 19, 10, 8] are effective. Recent studies have shown some success in applying CS to UQ problems [20, 64, 68, 33, 63, 51, 44, 32, 2]. For example, sampling strategies [48, 26, 3, 29] can improve the property of Ψ to guarantee sparse recovery via the ℓ_1 minimization. Computationally, the weighted ℓ_1 minimization [13, 68, 43, 49, 1] assigns larger weights to smaller components (in magnitude) of the solution, and hence minimizing the weighted ℓ_1 norm leads to a sparser solution than the vanilla ℓ_1 minimization does. Besides, adaptive basis selection [28, 16, 6, 3, 27] as well as dimension reduction techniques can be adopted to reduce the number of unknown [71, 58] thus improving computational efficiency.

In this paper, we focus on a sparsity-enhancing approach, e.g., iterative rotation [33, 69, 70, 72], that intrinsically changes the structure of the surrogate model to make the gPC coefficients more sparse. However, this method tends to deteriorate properties of Ψ that are favorable by CS algorithms, e.g., low coherence, which may counteract the benefit of the enhanced sparsity. Since the polynomials associated with the random variables may not be orthogonal after the rotation, the coherence of Ψ does not converges to zeros asymptotically, leading to an amplified coherence after the rotation. To remedy this drawback, we innovatively combine the iterative rotation technique with an ℓ_1 - ℓ_2 minimization algorithm [36, 74, 65] in order to improve the efficiency of CS-based UQ methods. Specifically, our new approach uses rotations to increase the sparsity while taking advantages of ℓ_1 - ℓ_2 formalism for dealing with Ψ that has a large mutual coherence. In this way, we leverage the advantages of both methods to exploit information from limited samples of the QoI more efficiently, and to construct gPC expansions more accurately.

The rest of the paper is organized as follows. We briefly review gPC, CS, and rotational CS in Section 2. We describe the combination of rotational CS and the ℓ_1 - ℓ_2 minimization in Section 3, followed by theoretical analysis on an upper bound of the change in coherence for a special case in Section 4. Section 5 devotes to extensive experimental results, showing that the proposed approach significantly outperforms the state-of-the-art. Finally, conclusions are given in Section 6.

2 Prior works

In this section, we briefly review gPC expansions, some useful concepts in CS, and a prior work on the rotational CS for gPC method.

2.1 Generalized polynomial chaos expansions

Given a set of N deterministic functions $\{c_n\}$ and multivariate polynomials $\{\psi_n\}$, a gPC expansion takes the following general form:

$$u(\mathbf{x}, t; \boldsymbol{\xi}) = \sum_{n=1}^N c_n(\mathbf{x}, t) \psi_n(\boldsymbol{\xi}) + \varepsilon(\mathbf{x}, t; \boldsymbol{\xi}), \quad (1)$$

where u is the QoI depending on location \mathbf{x} , time t and a set of random variables $\boldsymbol{\xi}$, and ε denotes any truncation error. Of particular interest is the case when $\{\psi_n\}_{n=1}^N$ are orthonormal with respect to the measure of $\boldsymbol{\xi}$, i.e.,

$$\int_{\mathbb{R}^d} \psi_i(\mathbf{x}) \psi_j(\mathbf{x}) \rho_{\boldsymbol{\xi}}(\mathbf{x}) d\mathbf{x} = \delta_{ij}, \quad (2)$$

where $\rho_{\boldsymbol{\xi}}(\mathbf{x})$ is the PDF of $\boldsymbol{\xi}$ and δ_{ij} is the Kronecker delta function. In this paper, we study systems relying on d -dimensional i.i.d. random variables $\boldsymbol{\xi} = (\xi_1, \dots, \xi_d)$, and the gPC basis functions are constructed by tensor products of univariate orthonormal polynomials. Specifically, for a multi-index $\boldsymbol{\alpha} = (\alpha_1, \dots, \alpha_d)$ with

each $\alpha_i \in \mathbb{N} \cup \{0\}$, we set

$$\psi_{\boldsymbol{\alpha}}(\boldsymbol{\xi}) = \psi_{\alpha_1}(\xi_1)\psi_{\alpha_2}(\xi_2)\cdots\psi_{\alpha_d}(\xi_d), \quad (3)$$

where ψ_{α_i} are univariate orthonormal polynomial of degree α_i . For two different multi-indices $\boldsymbol{\alpha} = (\alpha_1, \dots, \alpha_d)$ and $\boldsymbol{\beta} = (\beta_1, \dots, \beta_d)$, we have

$$\int_{\mathbb{R}^d} \psi_{\boldsymbol{\alpha}}(\mathbf{x})\psi_{\boldsymbol{\beta}}(\mathbf{x})\rho_{\boldsymbol{\xi}}(\mathbf{x})d\mathbf{x} = \delta_{\boldsymbol{\alpha}\boldsymbol{\beta}} = \delta_{\alpha_1\beta_1}\delta_{\alpha_2\beta_2}\cdots\delta_{\alpha_d\beta_d}, \quad (4)$$

where

$$\rho_{\boldsymbol{\xi}}(\mathbf{x}) = \rho_{\xi_1}(x_1)\rho_{\xi_2}(x_2)\cdots\rho_{\xi_d}(x_d). \quad (5)$$

Typically, a p th order gPC expansion involves all polynomials $\psi_{\boldsymbol{\alpha}}$ satisfying $|\boldsymbol{\alpha}| \leq p$, where $|\boldsymbol{\alpha}| = \sum_{i=1}^d \alpha_i$. This condition indicates that a total number of $N = \binom{p+d}{d}$ polynomials are used in the expansion. For simplicity, we reorder $\boldsymbol{\alpha}$ in such a way that we index $\psi_{\boldsymbol{\alpha}}$ by ψ_n , which is consistent with Eq. (1).

In this paper, we focus on time independent problems, in which the gPC expansion at a fixed location \mathbf{x} is given by

$$u(\boldsymbol{\xi}^q) = \sum_{n=1}^N c_n \psi_n(\boldsymbol{\xi}^q) + \varepsilon(\boldsymbol{\xi}^q), \quad q = 1, 2, \dots, M. \quad (6)$$

We rewrite the above expansion in terms of the matrix-vector notation, i.e.,

$$\boldsymbol{\Psi}\mathbf{c} = \mathbf{u} - \boldsymbol{\varepsilon}, \quad (7)$$

where $\mathbf{u} = (u^1, \dots, u^M)^\top$ is a vector of output samples, $\mathbf{c} = (c_1, \dots, c_N)^\top$ is a vector of gPC coefficients, measurement matrix $\boldsymbol{\Psi}$ is an $M \times N$ matrix with $\Psi_{ij} = \psi_j(\boldsymbol{\xi}^i)$ and $\boldsymbol{\varepsilon} = (\varepsilon^1, \dots, \varepsilon^M)^\top$ is a vector of error samples with $\varepsilon^q = \varepsilon(\boldsymbol{\xi}^q)$. We consider to solve an under-determined system with $M < N$ in (7), specifically interested in identifying sparse coefficients $\mathbf{c} = (c_1, \dots, c_N)^\top$, which is the focus of compressive sensing [17, 12, 22].

2.2 Compressive sensing

We review the concept of *sparsity*, which plays an important role in error estimation for solving the under-determined system (7). The number of non-zero entries of a vector $\mathbf{x} = (x_1, \dots, x_N)$ is denoted by $\|\mathbf{x}\|_0$ [17, 11, 8]. Note that $\|\cdot\|_0$ is named the “ ℓ_0 norm” in [17], although it is not a norm nor a semi-norm. The vector \mathbf{x} is called *s-sparse* if $\|\mathbf{x}\|_0 \leq s$, and it is considered a sparse vector if $s \ll N$. Few practical systems have truly sparse gPC coefficients, but rather compressible, i.e., only a few entries contributing significantly to its ℓ_1 norm. To this end, we define a vector \mathbf{x}_s as the best s -sparse approximation that can be obtained by setting all but the s -largest entries in magnitude of \mathbf{x} to zero. Subsequently, we call \mathbf{x} sparse or compressible if $\|\mathbf{x} - \mathbf{x}_s\|_1$ is small for $s \ll N$.

In order to find a sparse vector \mathbf{c} from (7), one formulates the following problem,

$$\hat{\mathbf{c}}_0 = \arg \min_{\mathbf{c}} \frac{1}{2} \|\boldsymbol{\Psi}\mathbf{c} - \mathbf{u}\|_2^2 + \lambda \|\mathbf{c}\|_0, \quad (8)$$

where λ is a positive parameter to be tuned such that $\|\boldsymbol{\Psi}\hat{\mathbf{c}}_0 - \mathbf{u}\|_2 \leq \epsilon$. As the ℓ_0 minimization (8) is NP-hard to solve [41], one often uses the convex ℓ_1 norm to replace ℓ_0 , i.e.,

$$\hat{\mathbf{c}}_1 = \arg \min_{\mathbf{c}} \frac{1}{2} \|\boldsymbol{\Psi}\mathbf{c} - \mathbf{u}\|_2^2 + \lambda \|\mathbf{c}\|_1. \quad (9)$$

A sufficient condition of the ℓ_1 minimization to exactly recover the sparse signal was proved based on the *restricted isometry property* (RIP) [11]. Unfortunately, RIP is numerically unverifiable for a given matrix [5, 56]. Instead, a computable condition for ℓ_1 's exact recovery is *coherence*, which is defined as

$$\mu(\boldsymbol{\Psi}) = \max_{i \neq j} \frac{|\langle \boldsymbol{\psi}_i, \boldsymbol{\psi}_j \rangle|}{\|\boldsymbol{\psi}_i\| \|\boldsymbol{\psi}_j\|}, \quad \text{with } \boldsymbol{\Psi} = [\boldsymbol{\psi}_1, \dots, \boldsymbol{\psi}_d]. \quad (10)$$

Donoho-Elad [18] and Gribonval [24] proved independently that if

$$\|\hat{\mathbf{c}}_1\|_0 < \frac{1}{2} \left(1 + \frac{1}{\mu(\Psi)} \right), \quad (11)$$

then $\hat{\mathbf{c}}_1$ is indeed the sparsest solution to (9). Apparently if the samples ξ^q are drawn independently, $\mu(\Psi)$ for the gPC expansion converges to zeros as $M \rightarrow \infty$ according to the distribution of ξ . However, the inequality (11) implies that the ℓ_1 minimization may not work well when the coherence of the matrix Ψ is large, e.g., $\mu(\Psi) \approx 1$, as (11) can only guarantee to recover a 1-sparse vector via the ℓ_1 minimization (9). Empirically speaking, the ℓ_1 minimization does not work very well when the matrix is coherent (i.e., μ is large). There are many nonconvex alternatives to approximate the ℓ_0 norm, including ℓ_p [14, 62, 31], capped ℓ_1 [77, 52, 37], transformed ℓ_1 [38, 75, 76], and ℓ_1/ℓ_2 [47, 59, 54]. In this work, we adopt the ℓ_1 - ℓ_2 functional [73, 36, 35] due to its outstanding performance in the coherent regime. Specifically, a recent work [25] reported that ℓ_1 - ℓ_2 is better than the weighted ℓ_1 minimization [13] for solving the ℓ_0 minimization.

2.3 Rotational compressive sensing

To further exploit sparsity, we aim to find a linear map $A : \mathbb{R}^d \mapsto \mathbb{R}^d$ such that a new set of random variables η , given by

$$\eta = \mathbf{A}\xi, \quad \eta = (\eta_1, \eta_2, \dots, \eta_d)^\top, \quad (12)$$

leads to a sparser polynomial expansion than ξ does. We consider \mathbf{A} as an orthogonal matrix, i.e., $\mathbf{A}\mathbf{A}^\top = \mathbf{I}$ with the identity matrix \mathbf{I} , such that the linear map from ξ to η can be regarded as a rotation in \mathbb{R}^d . Therefore, the new polynomial expansion for u is expressed as

$$u(\xi) \approx u_g(\xi) = \sum_{n=1}^N \tilde{c}_n \psi_n(\mathbf{A}\xi) = \sum_{n=1}^N \tilde{c}_n \psi_n(\eta) = v_g(\eta). \quad (13)$$

Here $u_g(\xi)$ can be understood as a polynomial $u_g(\mathbf{x})$ evaluated at random variables ξ , and the same for v_g . Ideally, $\tilde{\mathbf{c}}$ is sparser than \mathbf{c} . In the previous works [33, 69], it is assumed that $\xi \sim \mathcal{N}(\mathbf{0}, \mathbf{I})$, so $\eta \sim \mathcal{N}(\mathbf{0}, \mathbf{I})$. For general cases where $\{\xi_i\}_{i=1}^d$ are not i.i.d. Gaussian, $\{\eta_i\}_{i=1}^d$ are not necessarily independent. Moreover, $\{\psi_n\}_{n=1}^N$ are not necessarily orthogonal to each other with respect to ρ_η . Therefore, $v_g(\eta)$ may not be a standard gPC expansion of $v(\eta)$, but rather a polynomial equivalent to $u_g(\xi)$ with potentially sparser coefficients [72].

We can identify \mathbf{A} using the gradient information of u based on the framework of active subspace [50, 15]. In particular, we define

$$\mathbf{W} = \frac{1}{\sqrt{M}} [\nabla u(\xi^1), \nabla u(\xi^2), \dots, \nabla u(\xi^M)]. \quad (14)$$

Note that \mathbf{W} is a $d \times M$ matrix, and we consider $M \geq d$ in this work. The singular value decomposition (SVD) or principle component analysis (PCA) of \mathbf{W} yields

$$\mathbf{W} = \mathbf{U}\Sigma\mathbf{V}^\top, \quad (15)$$

where \mathbf{U} is a $d \times d$ orthogonal matrix, Σ is a $d \times M$ matrix, whose diagonal consists of singular values $\sigma_1 \geq \dots \geq \sigma_d \geq 0$, and \mathbf{V} is a $M \times M$ orthogonal matrix. We set the rotation matrix as $\mathbf{A} = \mathbf{U}^\top$. As such, the rotation projects ξ to the directions of principle components of ∇u . Of note, we do not use the information of the orthogonal matrix \mathbf{V} .

Unfortunately, u is unknown and samples of ∇u are not available. Instead of u , we approximate Eq. (14) by a computed solution u_g that can be obtained by standard ℓ_1 [69]. In other words, we have

$$\mathbf{W} \approx \mathbf{W}_g = \frac{1}{\sqrt{M}} [\nabla u_g(\xi^1), \nabla u_g(\xi^2), \dots, \nabla u_g(\xi^M)], \quad (16)$$

and the rotation matrix is constructed based on the SVD of \mathbf{W}_g :

$$\mathbf{W}_g = \mathbf{U}_g \mathbf{\Sigma}_g \mathbf{V}_g^\top, \quad \mathbf{A} = \mathbf{U}_g^\top. \quad (17)$$

Defining $\boldsymbol{\eta} = \mathbf{A}\boldsymbol{\xi}$, we compute the corresponding input samples as $\boldsymbol{\eta}^q = \mathbf{A}\boldsymbol{\xi}^q$ and construct a new measurement matrix $\boldsymbol{\Psi}(\boldsymbol{\eta})$ as $(\boldsymbol{\Psi}(\boldsymbol{\eta}))_{ij} = \psi_j(\boldsymbol{\eta}^i)$. We then solve the minimization problem in Eq. (9) to obtain $\tilde{\mathbf{c}}$. If some singular values of \mathbf{W} are much larger than the others, we can expect to obtain a sparser representation of \mathbf{u} with respect to $\boldsymbol{\eta}$, which is dominated by the eigenspace associated with these larger singular values. On the other hand, if all the singular values σ_i are of the same order, the rotation does not enhance the sparsity. In practice, this method can be designed as an iterative algorithm, in which \mathbf{A} and $\tilde{\mathbf{c}}$ are updated separately in each iteration following an alternating direction manner.

It is worth noting that the idea of using a linear map is also used in sliced inverse regression (SIR) [34], active subspace [50, 15], basis adaptation [57], etc., but with different manners in computing the matrix. In contrast to these methods, the iterative rotation approach does not truncate the dimension in the sense that \mathbf{A} is a square matrix. As an initial guess may not be sufficiently accurate, reducing dimension before the iterations terminate may lead to suboptimal results. The dimension reduction was integrated with the iterative method in [66], while another iterative rotation method preceded with SIR-based dimension reduction was proposed in [71]. We refer interested readers to the respective literature.

3 The proposed approach

When applying the rotational CS techniques, the measurement matrix $\boldsymbol{\Psi}(\boldsymbol{\eta})$ may become more coherent compared with $\boldsymbol{\Psi}$. This is because popular ψ_i used in gPC method, e.g., Legendre and Laguerre polynomials, are not orthogonal with respect to the measure of $\boldsymbol{\eta}$, so $\mu(\boldsymbol{\Psi}(\boldsymbol{\eta}))$ converges to a positive number instead of zeros as $\mu(\boldsymbol{\Psi})$ does. Under such coherent regime, we adopt the ℓ_1 - ℓ_2 minimization to identify the sparse coefficients $\tilde{\mathbf{c}}$.

To start with, we generate input samples $\{\boldsymbol{\xi}^q\}_{q=1}^M$ based on the distribution of $\boldsymbol{\xi}$ and select the gPC basis functions $\{\psi_j\}_{j=1}^N$ associated with $\boldsymbol{\xi}$ in order to generate the measurement matrix $\boldsymbol{\Psi}$ by setting $\Psi_{ij} = \psi_j(\boldsymbol{\xi}^i)$, where we initialize $\mathbf{A}^{(0)} = \mathbf{I}$ and $\boldsymbol{\eta}^{(0)} = \boldsymbol{\xi}$. Then we propose an alternating direction method (ADM) that combines the ℓ_1 - ℓ_2 minimization and rotation matrix estimation. Specifically given $\{\boldsymbol{\xi}^q\}_{q=1}^M$, $\{\psi_j\}_{j=1}^N$, and $\mathbf{u} := \{\mathbf{u}^q = u(\boldsymbol{\xi}^q)\}_{q=1}^M$, we formulate the following minimization problem,

$$\arg \min_{\mathbf{c}, \mathbf{A}} \frac{1}{2} \|\boldsymbol{\Psi}\mathbf{c} - \mathbf{u}\|_2^2 + \lambda(\|\mathbf{c}\|_1 - \theta\|\mathbf{c}\|_2), \quad \mathbf{A}\mathbf{A}^\top = \mathbf{I} \text{ and } \Psi_{ij} = \psi_j(\mathbf{A}\boldsymbol{\xi}^i). \quad (18)$$

If $\theta = 0$, it reduces to the ℓ_1 approach [69], while we propose to use $\theta = 1$ for the ℓ_1 - ℓ_2 model in this paper. We can minimize Eq. (18) with respect to \mathbf{c} and \mathbf{A} in an alternating direction manner. Specifically when \mathbf{A} is fixed, we minimize the ℓ_1 - ℓ_2 functional to identify \mathbf{c} , as detailed in Section 3.1. When \mathbf{c} is fixed, optimizing \mathbf{A} is computationally expensive, unless a dimension reduction technique is used, e.g., as in [58]. Instead, we use the rotation estimation introduced in Section 2.3 to compute \mathbf{A} . Admittedly, this way of estimating \mathbf{A} may not be optimal, but it promotes the sparsity of \mathbf{c} , thus improving the accuracy of the sparse approximation of the gPC expansion. In addition, the sparsity structure is problem-dependent (see examples in Section 5), and more iterations do not grant significant improvements for many practical problems.

3.1 ℓ_1 - ℓ_2 minimization

We focus on the \mathbf{c} -subproblem in (18), whose objective function is defined as

$$F(\mathbf{c}) = \frac{1}{2} \|\boldsymbol{\Psi}\mathbf{c} - \mathbf{u}\|_2^2 + \lambda(\|\mathbf{c}\|_1 - \theta\|\mathbf{c}\|_2).$$

We adopt the difference of convex algorithm (DCA) [45, 46] that decomposes $F(\mathbf{c}) = G(\mathbf{c}) - H(\mathbf{c})$ into

$$\begin{cases} G(\mathbf{c}) = \frac{1}{2} \|\boldsymbol{\Psi}\mathbf{c} - \mathbf{u}\|_2^2 + \lambda\|\mathbf{c}\|_1 \\ H(\mathbf{c}) = \lambda\theta\|\mathbf{c}\|_2. \end{cases}$$

An iterative scheme of minimizing $F(\mathbf{c})$ relies on a linearization of $H(\mathbf{c})$ at the current step $\mathbf{c}^{(n)}$ to advance to the next one, i.e.,

$$\mathbf{c}^{(n+1)} = \arg \min_{\mathbf{c} \in \mathbb{R}^n} \frac{1}{2} \|\Psi \mathbf{c} - \mathbf{u}\|_2^2 + \lambda \|\mathbf{c}\|_1 - \left\langle \mathbf{c}, \frac{\lambda \theta \mathbf{c}^{(n)}}{\|\mathbf{c}^{(n)}\|_2} \right\rangle. \quad (19)$$

Note that (19) is an ℓ_1 type of problems, which can be minimized by the alternating direction method of multipliers (ADMM) [7]. Denote $\mathbf{v} = \frac{\lambda \theta \mathbf{c}^{(n)}}{\|\mathbf{c}^{(n)}\|_2}$. We introduce an auxiliary variable \mathbf{y} and rewrite (19) as an equivalent problem,

$$\min_{\mathbf{c}, \mathbf{y}} \lambda \|\mathbf{c}\|_1 + \frac{1}{2} \|\Psi \mathbf{y} - \mathbf{u}\|_2^2 - \langle \mathbf{y}, \mathbf{v} \rangle. \quad \text{s.t.} \quad \mathbf{c} = \mathbf{y}. \quad (20)$$

This new formulation (20) makes the objective function separable with respect to two variables \mathbf{c} and \mathbf{y} . Specifically, the augmented Lagrangian corresponding to (20) can be expressed as

$$L_\rho(\mathbf{c}, \mathbf{y}; \mathbf{w}) = \lambda \|\mathbf{c}\|_1 + \frac{1}{2} \|\Psi \mathbf{y} - \mathbf{u}\|_2^2 - \langle \mathbf{y}, \mathbf{v} \rangle + \mathbf{w}^T (\mathbf{c} - \mathbf{y}) + \frac{\rho}{2} \|\mathbf{c} - \mathbf{y}\|_2^2, \quad (21)$$

where \mathbf{w} is an Lagrangian multiplier and ρ is a positive parameter. Then ADMM consists of three steps:

$$\mathbf{c}_{k+1}^{(n)} = \arg \min_{\mathbf{c}} \lambda \|\mathbf{c}\|_1 + \frac{\rho}{2} \|\mathbf{c} - \mathbf{y}_k^{(n)} + \frac{\mathbf{w}_k^{(n)}}{\rho}\|_2^2 \quad (22)$$

$$\mathbf{y}_{k+1}^{(n)} = \arg \min_{\mathbf{y}} \frac{1}{2} \|\Psi \mathbf{y} - \mathbf{u}\|_2^2 - \langle \mathbf{y}, \mathbf{v} \rangle + \frac{\rho}{2} \|\mathbf{c}_{k+1}^{(n)} - \mathbf{y} + \frac{\mathbf{w}_k^{(n)}}{\rho}\|_2^2 \quad (23)$$

$$\mathbf{w}_{k+1}^{(n)} = \mathbf{w}_k^{(n)} + \rho(\mathbf{c}_{k+1}^{(n)} - \mathbf{y}_{k+1}^{(n)}). \quad (24)$$

Here we use subscript k to indicate the inner ADMM iteration, as opposed to the superscript n for the outer DCA loop. The \mathbf{c} -update (22) has a closed-form solution given by

$$\mathbf{c}_{k+1}^{(n)} = \text{shrink}(\mathbf{y}_k^{(n)} - \frac{\mathbf{w}_k^{(n)}}{\rho}, \frac{\lambda}{\rho}), \quad (25)$$

where the *soft thresholding* or *shrinkage* is defined as

$$\text{shrink}(\mathbf{v}, \mu) = \begin{cases} \mathbf{v} - \mu & \mathbf{v} > \mu \\ 0 & |\mathbf{v}| \leq \mu \\ \mathbf{v} + \mu & \mathbf{v} < -\mu. \end{cases} \quad (26)$$

As for the \mathbf{y} -update (23), we take the gradient of L_ρ with respect to \mathbf{y} , thus leading to

$$\Psi^T (\Psi \mathbf{y} - \mathbf{u}) - \mathbf{v}^T + \rho(\mathbf{y} - \mathbf{c}_{k+1}^{(n)} - \frac{\mathbf{w}_k^{(n)}}{\rho}) = \mathbf{0}. \quad (27)$$

Therefore, the update for \mathbf{y} is given by

$$\mathbf{y}_{k+1}^{(n)} = (\Psi^T \Psi + \rho \mathbf{I})^{-1} \left(\Psi^T \mathbf{u} + \mathbf{v}^T + \rho \mathbf{c}_{k+1}^{(n)} + \mathbf{w}_k^{(n)} \right). \quad (28)$$

Note that $\Psi^T \Psi + \rho \mathbf{I}$ is a positive definite matrix and there are many efficient numeral algorithms for matrix inversion. Since Ψ has more columns than rows in our case, we further use the *Woodbury formula* to speed up,

$$\rho(\Psi^T \Psi + \rho \mathbf{I})^{-1} = \mathbf{I} - \frac{1}{\rho} \Psi^T (\Psi \Psi^T + \rho \mathbf{I})^{-1}, \quad (29)$$

as $\Psi \Psi^T$ has a smaller dimension than $\Psi^T \Psi$ to be inverted.

In summary, the overall ℓ_1 - ℓ_2 minimization algorithm is described in Algorithm 1.

Algorithm 1 ℓ_1 - ℓ_2 minimization via DCA

```
1: Input: measurement matrix  $\Psi$  and observed data  $\mathbf{u}$ .
2: Parameters:  $\lambda, \rho, \epsilon \in \mathbb{R}^+$  and  $n_{\max}, k_{\max} \in \mathbb{Z}^+$ .
3: Initialize:  $\mathbf{c}, \mathbf{y}, \mathbf{v}, \mathbf{w}$  and  $n, k = 0$ .
4: while  $n \leq n_{\max}$  or  $\|\mathbf{c}^{(n)} - \mathbf{c}^{(n-1)}\| > \epsilon$  do
5:    $\mathbf{v} = \lambda \theta \mathbf{c}^{(n)} / \|\mathbf{c}^{(n)} + \epsilon\|$ 
6:   while  $k \leq k_{\max}$  or  $\|\mathbf{c}^{(n)} - \mathbf{c}^{(n-1)}\| > \epsilon$  do
7:      $\mathbf{c}_{k+1} = \text{shrink}(\mathbf{y}_k - \mathbf{w}_k / \rho, \lambda / \rho)$ 
8:      $\mathbf{y}_{k+1} = (\Psi^\top \Psi + \rho \mathbf{I})^{-1} (\Psi^\top \mathbf{u} + \mathbf{v}^\top + \rho \mathbf{c}_{k+1} + \mathbf{w}_k)$ 
9:      $\mathbf{w}_{k+1} = \mathbf{w}_k + \rho(\mathbf{c}_{k+1} - \mathbf{y}_{k+1})$ 
10:     $k = k + 1$ .
11:   end while
12:    $\mathbf{c}^{(n+1)} = \mathbf{c}_k$ 
13:    $n = n + 1$  and  $k = 0$ 
14: end while
15: return  $\mathbf{c} = \mathbf{c}^{(n+1)}$ .
```

3.2 Rotation matrix update

Suppose we obtain the gPC coefficients $\tilde{\mathbf{c}}^{(l)}$ at the l -th iteration via Algorithm 1 with $l \geq 1$. Given $v_g^{(l)}(\boldsymbol{\eta})$ with input samples $\{(\boldsymbol{\eta}^{(l)})^q\}_{q=1}^M$ for $(\boldsymbol{\eta}^{(l)})^q = \mathbf{A}^{(l-1)}(\boldsymbol{\eta}^{(l-1)})^q$, we collect the gradient of $v_g^{(l)}$, denoted by

$$\mathbf{W}_g^{(l)} = \frac{1}{\sqrt{M}} \left[\nabla_{\boldsymbol{\xi}} v_g^{(l)} \left((\boldsymbol{\eta}^{(l)})^1 \right), \dots, \nabla_{\boldsymbol{\xi}} v_g^{(l)} \left((\boldsymbol{\eta}^{(l)})^M \right) \right], \quad (30)$$

where $\nabla_{\boldsymbol{\xi}} \cdot = (\partial \cdot / \partial \xi_1, \partial \cdot / \partial \xi_2, \dots, \partial \cdot / \partial \xi_d)^\top$. It is straightforward to evaluate $\nabla \psi_n$ at $(\boldsymbol{\eta}^{(l)})^q$, as we construct ψ_n using the tensor product of univariate polynomials (3) and derivatives for widely used orthogonal polynomials, e.g., Hermite, Laguerre, Legendre, and Chebyshev, are well studied in the UQ literature. Here, we can analytically compute the gradient of $v_g^{(l)}$ with respect to $\boldsymbol{\xi}$ using the chain rule,

$$\begin{aligned} \nabla_{\boldsymbol{\xi}} v_g^{(l)} \left((\boldsymbol{\eta}^{(l)})^q \right) &= \nabla_{\boldsymbol{\xi}} v_g^{(l)} \left(\mathbf{A}^{(l)} \boldsymbol{\xi}^q \right) = \left(\mathbf{A}^{(l)} \right)^\top \nabla v_g^{(l)}(\mathbf{x}) \Big|_{\mathbf{x} = \mathbf{A}^{(l)} \boldsymbol{\xi}^q} \\ &= \left(\mathbf{A}^{(l)} \right)^\top \nabla \sum_{n=1}^N \tilde{c}_n^{(l)} \psi_n(\mathbf{x}) \Big|_{\mathbf{x} = \mathbf{A}^{(l)} \boldsymbol{\xi}^q} = \left(\mathbf{A}^{(l)} \right)^\top \sum_{n=1}^N \tilde{c}_n^{(l)} \nabla \psi_n(\mathbf{x}) \Big|_{\mathbf{x} = \mathbf{A}^{(l)} \boldsymbol{\xi}^q}. \end{aligned} \quad (31)$$

Then, we have an update for $\mathbf{A}^{(l+1)} = \left(\mathbf{U}_g^{(l)} \right)^\top$, where $\mathbf{U}_g^{(l)}$ is from the SVD of

$$\mathbf{W}_g^{(l)} = \mathbf{U}_g^{(l)} \boldsymbol{\Sigma}_g^{(l)} \left(\mathbf{V}_g^{(l)} \right)^\top. \quad (32)$$

Now we can define a new set of random variables as $\boldsymbol{\eta}^{(l+1)} = \mathbf{A}^{(l+1)} \boldsymbol{\xi}$ and compute their samples accordingly: $(\boldsymbol{\eta}^{(l+1)})^q = \mathbf{A}^{(l+1)} \boldsymbol{\xi}^q$. These samples will be used to construct a new measurement matrix $\Psi^{(l+1)}$ as $\Psi_{ij}^{(l+1)} = \psi_j((\boldsymbol{\eta}^{(l+1)})^i)$ to feed into the ℓ_1 - ℓ_2 minimization to obtain $\mathbf{c}^{(l+1)}$.

We summarize the entire procedure in Algorithm 2. The stopping criterion we use is $l \leq l_{\max}$, where l_{\max} is can taken as 2 or 3 empirically for practical problems. Alternatively, it can be set as the difference between two successive rotation matrices $\mathbf{A}^{(l)}$ and $\mathbf{A}^{(l+1)}$.

Algorithm 2 Alternating direction method of minimizing (18)

- 1: Generate input samples $\{\xi^q\}_{q=1}^M$ based on the distribution of ξ .
- 2: Generate corresponding output samples $\mathbf{u} := \{u^q = u(\xi^q)\}_{q=1}^M$ by solving the complete model, e.g., running simulations, solvers, etc.
- 3: Select gPC basis functions $\{\psi_n\}_{n=1}^N$ associated with ξ and set counter $l = 0$. Set $\mathbf{A}^{(0)} = \mathbf{I}$ and $\boldsymbol{\eta}^{(0)} = \xi$.
- 4: Generate the measurement matrix $\Psi^{(l)}$ by setting $\Psi_{ij}^{(l)} = \psi_j(\xi^i)$.
- 5: **for** $l < l_{\max}$ **do**
- 6: **if** $l > 0$ **then**
- 7: Construct $\mathbf{W}^{(l)}$ in (30) with $v_g^{(l)} = \sum_{n=1}^N \tilde{c}^{(l)} \psi_n(\xi^{(l)})$.
- 8: Compute SVD of $\mathbf{W}_g^{(l)}$: $\mathbf{W}_g^{(l)} = \mathbf{U}_g^{(l)} \boldsymbol{\Sigma}_g^{(l)} \left(\mathbf{V}_g^{(l)}\right)^\top$.
- 9: Set $\mathbf{A}^{(l+1)} = \left(\mathbf{U}_g^{(l)}\right)^\top$ and $\boldsymbol{\eta}^{(l+1)} = \mathbf{A}^{(l+1)} \xi$.
- 10: Construct the new measurement matrix $\Psi^{(l+1)}$ with $\Psi_{ij}^{(l+1)} = \psi_j((\boldsymbol{\eta}^{(l+1)})^i)$.
- 11: **end if**
- 12: Solve the ℓ_1 - ℓ_2 minimization via DCA (Algorithm 1):

$$\tilde{\mathbf{c}}^{(l+1)} = \arg \min_{\mathbf{c}} \frac{1}{2} \|\Psi^{(l+1)} \mathbf{c} - \mathbf{u}\|_2^2 + \lambda(\|\mathbf{c}\|_1 - \theta \|\mathbf{c}\|_2).$$

- 13: $l = l + 1$.
- 14: **end for**

- 15: Construct gPC expansion as $u(\xi) \approx u_g(\xi) = v_g^{(l_{\max})}(\boldsymbol{\eta}^{(l_{\max})}) = \sum_{n=1}^N \tilde{c}_n^{(l_{\max})} \psi_n(\mathbf{A}^{(l_{\max})} \xi)$.
-

4 Theoretical analysis

Generally speaking, $\psi_i(\mathbf{A}\mathbf{x})_{n=1}^N$ are not orthogonal with respect to the measure of ξ [72], i.e.,

$$\int_{\mathbb{R}^d} \psi_i(\mathbf{x}) \psi_j(\mathbf{x}) \rho_{\xi}(\mathbf{x}) d\mathbf{x} \neq \delta_{ij}. \quad (33)$$

As a result, the mutual coherence of matrix $\Psi(\boldsymbol{\eta})$ does not converge to zero as the number of samples increases. Besides, $\mu(\Psi(\boldsymbol{\eta}))$ can even be larger than $\mu(\Psi)$. An exception is the normalized Hermite polynomial associated with the standard normal random variables $\mathcal{N}(\mathbf{0}, \mathbf{I})$. Rotating a sample drawn from $\mathcal{N}(\mathbf{0}, \mathbf{I})$ still yields a sample of a standard normal random variable, so the expectation of the mutual coherence remain the same, i.e., $\mathbb{E}\{\mu(\Psi)\} = \mathbb{E}\{\mu(\Psi(\boldsymbol{\eta}))\}$. In practice, we draw a sample from the standard normal distribution, then accept this sample as ξ^i only if it is within a ball $B_R(0)$ with a radius parameter $R > 0$. As the samples ξ^i are drawn from a truncated normal distribution, Hermite polynomials are not necessarily orthonormal with respect to the measure of ξ . Theorem 4.3 provides an upper bound for the change of μ in the case of Hermite polynomials. To prove for Theorem 4.3, we introduce Lemma 4.1 that can be proved in the same way as in [20].

Lemma 4.1 *Let ξ^1, \dots, ξ^M be independent samples drawn from the truncated normal distribution, i.e., $\xi \sim \mathcal{N}(\mathbf{0}, \mathbf{I})$ with $\|\xi\|_2 < R$. $\{\psi_j\}_{j=1}^N$ are normalized multivariate Hermite polynomials constructed as in Eq. (3) with maximum order p , and a matrix Ψ is constructed as $\Psi_{ij} = \psi_j(\xi^i)$. Denote $\tau_{jk} = \mathbb{E}\{\psi_j(\xi) \psi_k(\xi)\}$ (for $j \neq k$), $\tau_{jj} = 1 - \mathbb{E}\{\psi_j^2(\xi)\}$, and $\tau = \max_{1 \leq j, k \leq N} |\tau_{jk}|$. Then for any $t > 0$,*

$$\text{Prob} \left\{ \mu(\Psi) \geq \frac{\tau + t}{1 - \tau - t} \right\} < 2N^2 \exp \left(-\frac{M(t + \tau)^2}{2C_1^2 R^{2p}} \right), \quad (34)$$

where C_1 is a constant depending on p .

Proof 4.2 It is clear that

$$\mathbb{E} \left\{ \frac{1}{M} \sum_{i=1}^M \psi_j(\boldsymbol{\xi}^i) \psi_k(\boldsymbol{\xi}^i) \right\} = \mathbb{E} \{ \psi_j(\boldsymbol{\xi}) \psi_k(\boldsymbol{\xi}) \} = \tau_{jk}, \quad j \neq k,$$

and

$$\mathbb{E} \left\{ \frac{1}{M} \sum_{i=1}^M \psi_j^2(\boldsymbol{\xi}^i) \right\} = \mathbb{E} \{ \psi_j^2(\boldsymbol{\xi}) \} = 1 - \tau_{jj}.$$

Using the McDiarmid's inequality [40], we obtain that for $t > 0$,

$$\text{Prob} \left\{ \left| \frac{1}{M} \sum_{i=1}^M \psi_j(\boldsymbol{\xi}^i) \psi_k(\boldsymbol{\xi}^i) - \tau_{jk} \right| \geq t \right\} \leq 2 \exp \left(-\frac{2Mt^2}{4H^2(R, p)} \right), \quad (35)$$

where $H(R, p) = \sup_{\mathbf{x} \in B_R(0)} |\psi_j(\mathbf{x})| \leq C_1 R^p$ with a constant C_1 that only depends on p . The inequality (35) indicates that

$$\text{Prob} \left\{ \left| \frac{1}{M} \sum_{i=1}^M \psi_j(\boldsymbol{\xi}^i) \psi_k(\boldsymbol{\xi}^i) \right| \geq \tau + t \right\} \leq 2 \exp \left(-\frac{Mt^2}{2H^2(R, p)} \right).$$

Similarly, we get

$$\text{Prob} \left\{ \frac{1}{M} \sum_{i=1}^M \psi_j^2(\boldsymbol{\xi}^i) \leq 1 - \tau - t \right\} \leq 2 \exp \left(-\frac{Mt^2}{2H^2(R, p)} \right).$$

The above two probability estimations yield that

$$\text{Prob} \left\{ \left| \frac{\frac{1}{M} \sum_{i=1}^M \psi_j(\boldsymbol{\xi}^i) \psi_k(\boldsymbol{\xi}^i)}{(\frac{1}{M} \sum_{i=1}^M \psi_j^2(\boldsymbol{\xi}^i))^{1/2} (\frac{1}{M} \sum_{i=1}^M \psi_k^2(\boldsymbol{\xi}^i))^{1/2}} \right| \geq \frac{\tau + t}{1 - \tau - t} \right\} \leq 4 \exp \left(-\frac{Mt^2}{2C_1^2 R^{2p}} \right).$$

Notice that

$$\mu(\boldsymbol{\Psi}) = \max_{\substack{1 \leq j, k \leq N \\ j \neq k}} \left| \frac{\frac{1}{M} \sum_{i=1}^M \psi_j(\boldsymbol{\xi}^i) \psi_k(\boldsymbol{\xi}^i)}{(\frac{1}{M} \sum_{i=1}^M \psi_j^2(\boldsymbol{\xi}^i))^{1/2} (\frac{1}{M} \sum_{i=1}^M \psi_k^2(\boldsymbol{\xi}^i))^{1/2}} \right|,$$

so

$$\text{Prob} \left\{ \mu(\boldsymbol{\Psi}) \geq \frac{\tau + t}{1 - \tau - t} \right\} \leq \binom{N}{2} 4 \exp \left(-\frac{Mt^2}{2C_1^2 R^{2p}} \right) < 2N^2 \exp \left(-\frac{M(t + \tau)^2}{2C_1^2 R^{2p}} \right).$$

Since $\|\mathbf{A}\boldsymbol{\xi}^i\|_2 = \|\boldsymbol{\xi}^i\|_2$ for a unitary matrix \mathbf{A} , Lemma 4.1 still holds when replacing $\boldsymbol{\xi}^i$ with $\mathbf{A}\boldsymbol{\xi}^i$. Therefore, we have the following theorem:

Theorem 4.3 Let $\{\boldsymbol{\xi}^i\}_{i=1}^M$ be independent samples of the normal random variable $\boldsymbol{\xi} \sim \mathcal{N}(\mathbf{0}, \mathbf{I})$ with $\|\boldsymbol{\xi}^i\|_2 < R$, \mathbf{A} is a unitary matrix, matrix $\tilde{\boldsymbol{\Psi}}$ is constructed as $\tilde{\Psi}_{ij} = \psi_j(\mathbf{A}\boldsymbol{\xi}^i)$, then we have

$$\text{Prob} \left\{ |\mu(\boldsymbol{\Psi}) - \mu(\tilde{\boldsymbol{\Psi}})| < \frac{r}{1 - r} \right\} > 1 - 4N^2 \exp \left(-\frac{Mr^2}{2C_1^2 R^{2p}} \right), \quad (36)$$

where $r = \tau + t \geq \tau$ and τ is defined in Lemma 4.1.

Proof 4.4 Apply Lemma 4.1 to $\mu(\boldsymbol{\Psi})$ and $\mu(\tilde{\boldsymbol{\Psi}})$, and use the fact that $\mu(\boldsymbol{\Psi}), \mu(\tilde{\boldsymbol{\Psi}}) \geq 0$.

5 Numerical Examples

In this section, we conduct extensive experiments using three different types of polynomial expansions to demonstrate the performance of the proposed method in comparison to the one without rotation (by setting $l_{\max} = 1$ in Algorithm 2) and the ℓ_1 approach (by setting $\theta = 1$ in (18)). The performance is evaluated in terms of relative error (RE), defined as $\frac{\|u - u_g\|_2}{\|u\|_2}$, where u is the exact solution, u_g is the gPC approximation of u , and the integral in computing the norm $\|\cdot\|_2$ is approximated with a high-level sparse grids method, based on one-dimensional Gaussian quadrature and the Smolyak structure [53].

The parameters λ, ρ for both ℓ_1 and ℓ_1 - ℓ_2 are tuned to achieve the smallest RE after $l_{\max} = 9$ rotations for demonstration purpose. In particular, we start with a coarser grid of $10^{-4}, 10^{-3}, \dots, 10^1$. Once we find the optimal order, we then multiply it by 0.5, 1, \dots , 9.5 to find the optimal values, denoted by $(\bar{\lambda}, \bar{\rho})$, that provide the smallest RE. Note that $(\bar{\lambda}, \bar{\rho})$ may not be optimal for other number of rotations, except for 9. We specify the optimal parameter pair $(\bar{\lambda}, \bar{\rho})$ for each testing case in the corresponding section. In practice, the parameters can be determined by cross-validation or followed by the work of [65].

5.1 Ridge function

Consider the following ridge function:

$$u(\xi) = \sum_{i=1}^d \xi_i + 0.25 \left(\sum_{i=1}^d \xi_i \right)^2 + 0.025 \left(\sum_{i=1}^d \xi_i \right)^3. \quad (37)$$

As $\{\xi_i\}_{i=1}^d$ are equally important in this example, adaptive methods [39, 67, 78] that build surrogate models hierarchically based on the importance of ξ_i may not be effective. We consider a rotation matrix in the form of

$$\mathbf{A} = \begin{pmatrix} d^{-\frac{1}{2}} & d^{-\frac{1}{2}} & \dots & d^{-\frac{1}{2}} \\ & \tilde{\mathbf{A}} & & \end{pmatrix}, \quad (38)$$

where $\tilde{\mathbf{A}}$ is an $d \times (d-1)$ matrix designed to guarantee the orthogonality of the matrix \mathbf{A} , e.g., \mathbf{A} can be obtained by the Gram-Schmidt process. With this choice of \mathbf{A} , we have $\eta_1 = d^{-\frac{1}{2}} \sum_{i=1}^d \xi_i$ and u can be represented as

$$u(\boldsymbol{\xi}) = v(\boldsymbol{\eta}) = d^{\frac{1}{2}} \eta_1 + 0.25 d \eta_1^2 + 0.025 d^{\frac{3}{2}} \eta_1^3. \quad (39)$$

In the expression $u(\boldsymbol{\xi}) = \sum_{n=1}^N \tilde{c}_n \psi_n(\mathbf{A}\boldsymbol{\xi}) = \sum_{n=1}^N \tilde{c}_n \psi_n(\boldsymbol{\eta})$, all of the polynomials that are not related to η_1 make no contribution to the expansion, which guarantees the sparsity of $\tilde{\mathbf{c}} = (\tilde{c}_1, \dots, \tilde{c}_N)$.

By setting $d = 12$ (hence, the number of gPC basis functions is $N = 455$ for $p = 3$), we compare the accuracy of computing gPC expansions using ℓ_1 and ℓ_1 - ℓ_2 minimization with and without rotations. We consider gPC expansion using Legendre polynomial (assuming ξ_i are i.i.d. uniform random variables), Hermite polynomial expansion (assuming ξ_i are i.i.d. Gaussian random variables), and Laguerre polynomial (assuming ξ_i are i.i.d. exponential random variables), respectively. The number of sample M ranges from 100 to 180 in our tests. Each experiment is repeated 100 times with 9 rotations for each case to compute the average RE. We choose the optimal parameters of $(\bar{\lambda}, \bar{\rho})$ to be $(3 \times 10^{-4}, 5 \times 10^{-1})$, $(10^{-4}, 10^{-2})$, and $(5 \times 10^{-1}, 1)$ for the ℓ_1 - ℓ_2 method, when considering Legendre, Hermite, and Laguerre polynomials, respectively. As for ℓ_1 , the optimal parameters $(\bar{\lambda}, \bar{\rho})$ are set as $(6 \times 10^{-4}, 6 \times 10^{-1})$, $(10^{-2}, 10^{-1})$, and $(5 \times 10^{-2}, 5)$, for the corresponding polynomials.

Figure 1 presents relative errors corresponding to different ratio M/N . It shows that the standard ℓ_1 minimization without rotation is not effective, as the relative error is close to 50% even when M/N approaches 0.4. On the other hand, the ℓ_1 - ℓ_2 approach does not improve much upon ℓ_1 in this case, but rather our

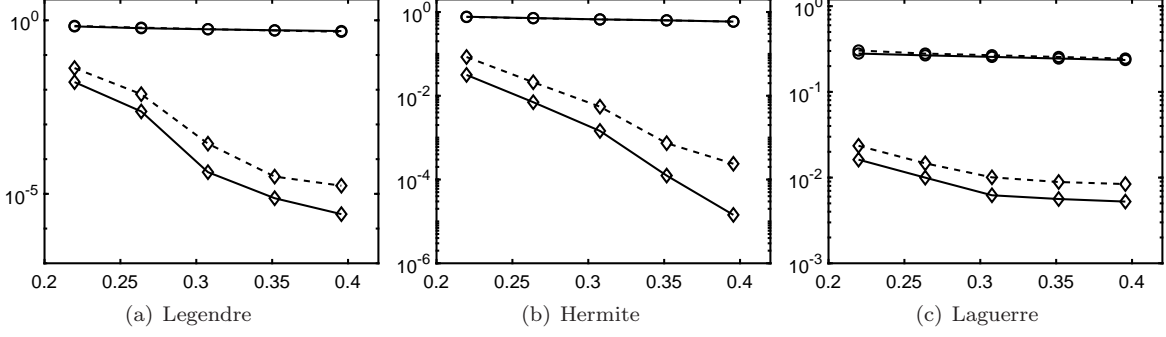


Figure 1: (Ridge function) Relative error of Legendre, Hermite and Laguerre polynomial expansions for ridge function against ratio M/N . Solid lines are for ℓ_1 - ℓ_2 minimization and dashed lines are for ℓ_1 minimization, while the marker “o” is used for results without rotation and “ \diamond ” for results with 9 rotations.

iterative rotation demonstrates much higher accuracy, especially when M is large. The reason can be partially explained by Figure 2. Specifically, Figure 2 (a), (b) and (c) plot the absolute values of exact coefficients $|c_n|$ of Legendre, Hermite, and Laguerre polynomials before rotation using 120 samples (randomly chosen from the 100 independent experiments), while Figure 2 (d), (e) and (f) show corresponding coefficients $|\tilde{c}_n|$ after 9 iterations. In Figure 2, we do not include \tilde{c}_n whose absolute value is smaller than 10^{-3} , since they are sufficiently small (more than two magnitudes smaller than the dominating ones). As demonstrated in Figure 2, the iterative updates on the rotation matrix significantly sparsifies the representation of u ; and as a result, the efficiency of compressive sensing methods is substantially enhanced.

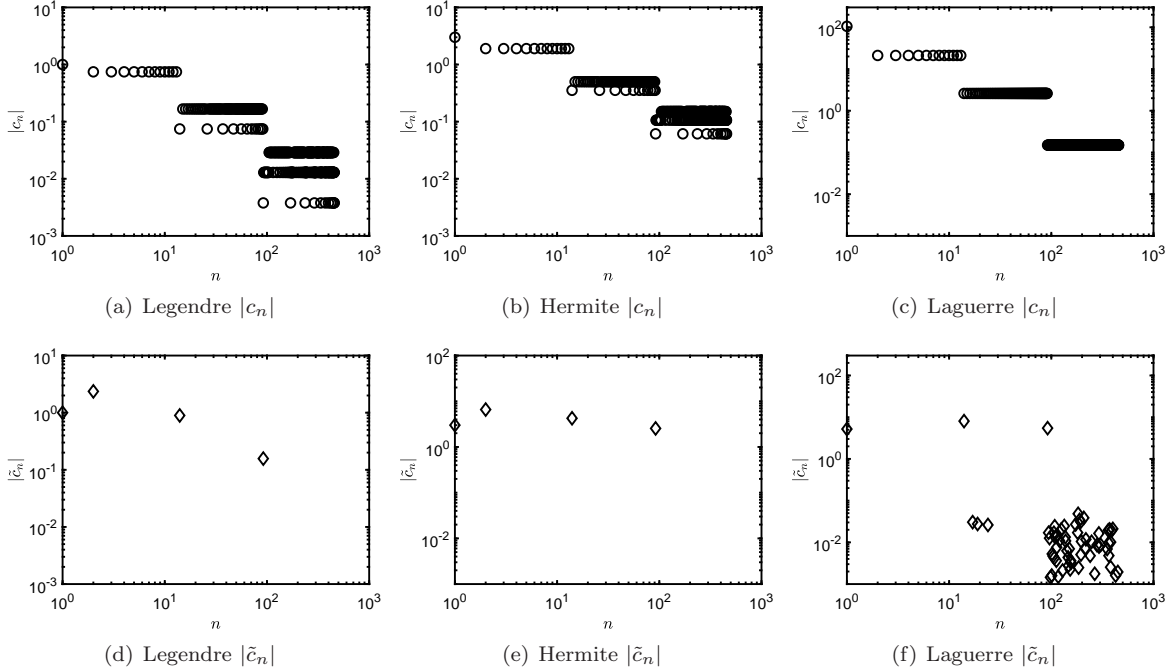


Figure 2: (Ridge function) Absolute values of exact coefficients c_n (first row) and coefficients \tilde{c}_n after 9 rotations (second row) using 120 samples.

5.2 Korteweg-de Vries equation

As an example of a more complicated and nonlinear differential equation, we consider the Korteweg-de Vries (KdV) equation with time-dependent additive noise,

$$\begin{aligned} u_t(x, t; \xi) - 6u(x, t; \xi)u_x(x, t; \xi) + u_{xxx}(x, t; \xi) &= f(t; \xi), \quad x \in (-\infty, \infty) \\ u(x, 0; \xi) &= -2 \operatorname{sech}^2(x). \end{aligned} \quad (40)$$

Here $f(t; \xi)$ is modeled as a random field represented by the Karhunen-Loève expansion:

$$f(t; \xi) = \sigma \sum_{i=1}^d \sqrt{\lambda_i} \phi_i(t) \xi_i, \quad (41)$$

where σ is a constant and $\{\lambda_i, \phi_i(t)\}_{i=1}^d$ are eigenvalues/eigenfunctions (in a descending order) of the exponential covariance kernel:

$$C(x, x') = \exp\left(-\frac{|x - x'|}{l_c}\right). \quad (42)$$

The value of $\{\lambda_i\}_{i=1}^d$ and analytical expressions for $\{\phi_i(x)\}_{i=1}^d$ are discussed in [30]. We set $l_c = 0.25$ and $d = 10$ in (42) such that $\sum_{i=1}^d \lambda_i > 0.96 \sum_{i=1}^{\infty} \lambda_i$. Under this setting, we have an analytical solution given by

$$u(x, t; \xi) = \sigma \sum_{i=1}^d \sqrt{\lambda_i} \xi_i \int_0^t \phi_i(y) dy - 2 \operatorname{sech}^2\left(x - 4t + 6\sigma \sum_{i=1}^d \sqrt{\lambda_i} \xi_i \int_0^t \int_0^z \phi_i(y) dy dz\right). \quad (43)$$

We choose QoI to be $u(x, t; \xi)$ at $x = 6, t = 1$, and $\sigma = 0.4$. Thanks to analytical expressions of $\phi_i(x)$, we can compute the integrals in (43) with high accuracy. Denote

$$A_i = \sqrt{\lambda_i} \int_0^1 \phi_i(y) dy \quad \text{and} \quad B_i = \sqrt{\lambda_i} \int_0^1 \int_0^z \phi_i(y) dy dz, \quad i = 1, 2, \dots, d, \quad (44)$$

the analytical solution can be written as

$$u(x, t; \xi)|_{x=6, t=1} = \sigma \sum_{i=1}^d A_i \xi_i - 2 \operatorname{sech}^2\left(2 + 6\sigma \sum_{i=1}^d B_i \xi_i\right). \quad (45)$$

We use a fourth-order gPC expansion to approximate the solution, i.e., $p = 4$, and the number of gPC basis functions $N = 1001$. The experiment is repeated 50 times with 3 rotations for each gPC expansion to compute the average relative error. For both polynomials, we fix $\bar{\lambda} = 1 \times 10^{-4}$ and $\bar{\rho} = 1 \times 10^{-2}$ in ℓ_1 - ℓ_2 , while choosing $(10^{-4}, 10^{-2})$, $(10^{-2}, 4 \times 10^{-4})$ in ℓ_1 for Legendre and Hermite, respectively. The relative errors of the Legendre and Hermite polynomial expansions are presented in Figure 3, which illustrates the combined method of iterative rotation and ℓ_1 - ℓ_2 minimization outperforms ℓ_1 and ℓ_1 - ℓ_2 approaches. In the Hermite polynomial case, when the sample size is small (i.e., $M/N \leq 0.12$), ℓ_1 - ℓ_2 alone can outperform the combination of ℓ_1 and iterative rotation method. This indicates that the impact of increased coherence after rotation on ℓ_1 minimization is more significant than the potential enhancement of sparsity. Similarly for the Legendre case, the ℓ_1 - ℓ_2 without rotation is close to ℓ_1 combined with rotation when $M/N = 0.1$.

5.3 High-dimensional function

We illustrate the potential capability of the proposed approach for dealing with higher-dimensional problems, referred to as HD function. Specifically, we select a function similar to the one in Section 5.1 but with a much higher dimension,

$$u(\xi) = \sum_{i=1}^d \xi_i + 0.25 \left(\sum_{i=1}^d \xi_i / \sqrt{i} \right)^2, \quad d = 100. \quad (46)$$

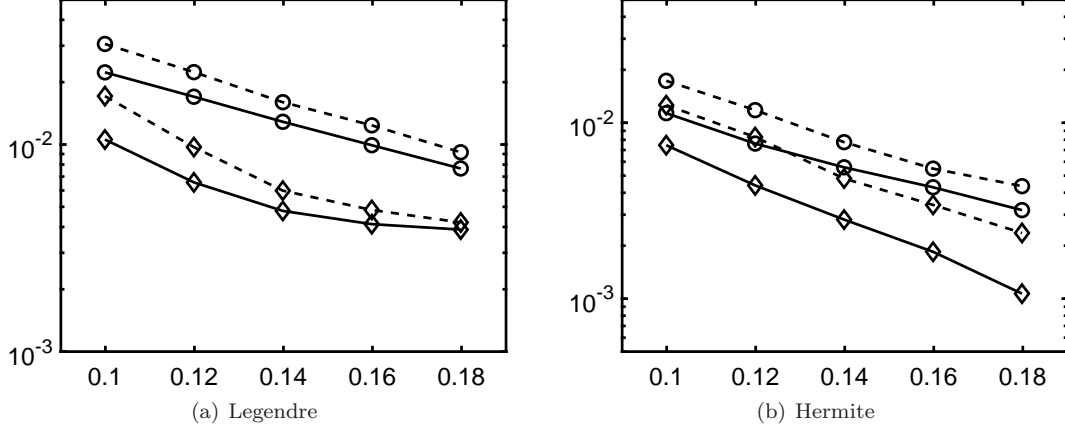


Figure 3: (KdV equation) Relative error of Legendre and Hermite polynomial expansions for KdV equation against ratio M/N . Solid lines are for ℓ_1 - ℓ_2 minimization and dashed lines are for ℓ_1 minimization. “o” is the marker for results without rotation and “ \diamond ” is the marker for results with 3 rotations.

The total number of basis functions for this example is $N = 5151$. The experiment is repeated 20 times with 3 rotations for each polynomial to compute the average relative error. We choose $(\bar{\lambda}, \bar{\rho})$ to be $(5 \times 10^{-2}, 5 \times 10^{-4})$ and $(10^{-3}, 9 \times 10^{-2})$ in ℓ_1 - ℓ_2 as well as $(1.2, 5 \times 10^{-2})$ and $(10^{-2}, 10^{-3})$ in ℓ_1 for Legendre and Hermite, respectively. The results are presented in Figure 4. As in the previous examples, ℓ_1 - ℓ_2 combined with rotation yields best results.

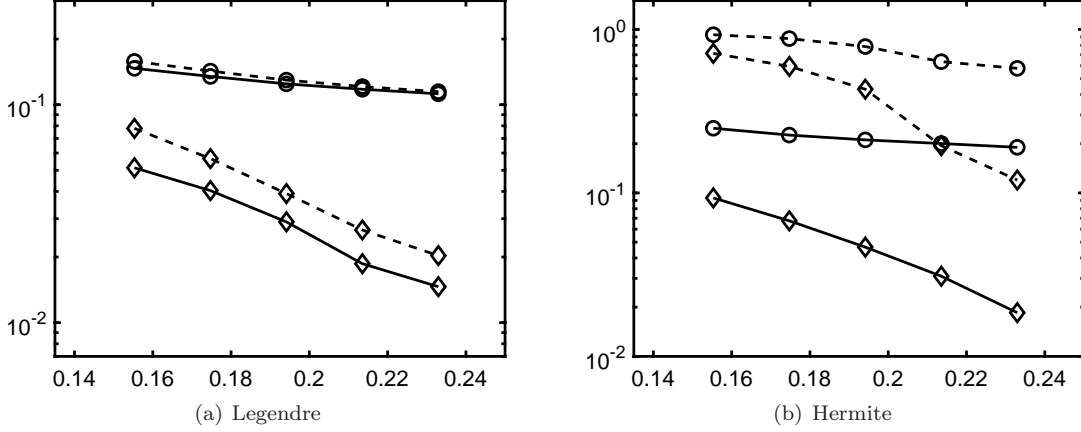


Figure 4: (High-dimensional function) Relative error of Legendre and Hermite polynomial expansions for the high-dimensional function. Solid lines are for ℓ_1 - ℓ_2 minimization and dashed lines are for ℓ_1 minimization. “o” is the marker for results without rotation and “ \diamond ” is the marker for results with 3 rotations.

5.4 Discussion

We intend to discuss the effects of coherence and the number of rotations on the performance of the ℓ_1 and ℓ_1 - ℓ_2 approaches. As reported in [74, 36], ℓ_1 - ℓ_2 performs particularly well for coherent matrices. The coherence values are reported in Tables 1-2 for ridge and KdV/HD, respectively. Both Tables 1-2 confirm that more rotations increase the coherence level of the sensing matrix Ψ except for the Hermite polynomial case. For relatively incoherent scenarios (e.g., Legendre and Hermite in Ridge), we observe significant

improvements of ℓ_1 - ℓ_2 over ℓ_1 in numerical simulations (see Figure 1). On the other hand, ℓ_1 - ℓ_2 is slightly better than ℓ_1 when coherence values are closer to 1 (e.g., Laguerre in Ridge), which seems difficult for any sparse recovery algorithms.

Table 1: Average coherence of matrix Ψ (size 160×455) for ridge function.

Rotations	Ridge function		
	Legendre	Hermite	Laguerre
0	0.4692	0.7622	0.9448
3	0.6833	0.7527	0.9910
6	0.6822	0.7519	0.9911
9	0.6762	0.7657	0.9911

Table 2: Average coherence of matrix Ψ for KdV (matrix size 160×1001) and HD function (matrix size 1000×5151).

Rotations	KdV equation		HD function	
	Legendre	Hermite	Legendre	Hermite
0	0.6079	0.9121	0.2117	0.2852
1	0.8825	0.9223	0.2580	0.3075
2	0.8487	0.9167	0.2664	0.2956
3	0.8677	0.9214	0.2522	0.3003

The effect of the number of rotations is examined in Figure 5. For Ridge function, more rotations lead to a better accuracy, while it stagnates at 3-5 rotations for the KdV equation. This is because the ridge function has very good low-dimensional structure, i.e., the dimension can be reduced to one using a linear transformation $\eta = \xi$, while the KdV equation does not have this property. Also, there is no truncation error $\varepsilon(\xi)$ when using the gPC expansion to represent the ridge function as we use a third order expansion, while $\varepsilon(\xi)$ exists for the KdV equation. In most practical problems, the truncation error exists and the linear transform may not yield a very good low-dimensional structure to have sparse coefficients of the gPC expansion. Therefore, we empirically set a maximum number of rotations l_{\max} to terminate iterations in the algorithm.

Finally, we present the computation time in Table 3. All the experiments are performed on an AMD Ryzen 5 3600, 16 GB RAM machine on Windows 10 system with Matlab 2018b. The major computation comes from two components: one is the ℓ_1 - ℓ_2 minimization and the other is to find the rotation matrix A . The computation complexity for every iteration of the ℓ_1 - ℓ_2 algorithm is $O(M^3 + M^2N)$, which reduces to $O(M^2N)$ as we assume $M \ll N$. In practice, we choose the maximum outer/inner numbers in Algorithm 1 as $n_{\max} = 10, k_{\max} = 2N$ respectively, and hence the complexity for ℓ_1 - ℓ_2 algorithm is $O(M^2N^2)$. To find the rotation matrix A , one has to construct a matrix W using (30) with complexity of $O(M^3N)$, followed by SVD with complexity of $O(M^3N + M^2N^2)$. Therefore, the total complexity of our approach is $O(M^2N^2)$ per rotation. We divide the time of Legendre polynomial reported in Table 3 by $l_{\max}(MN)^2$, getting $1.39e^{-10}, 1.95e^{-10}$, and $0.25e^{-10}$. As the ratios are of the same order, the empirical results are consistent with the complexity analysis.

6 Conclusions

In this work, we proposed an alternating direction method to identify a rotation matrix iteratively in order to enhance the sparsity of gPC expansion, followed by the ℓ_1 - ℓ_2 minimization to efficiently identify the sparse coefficients. As such, it improves the accuracy of the compressive sensing method to construct

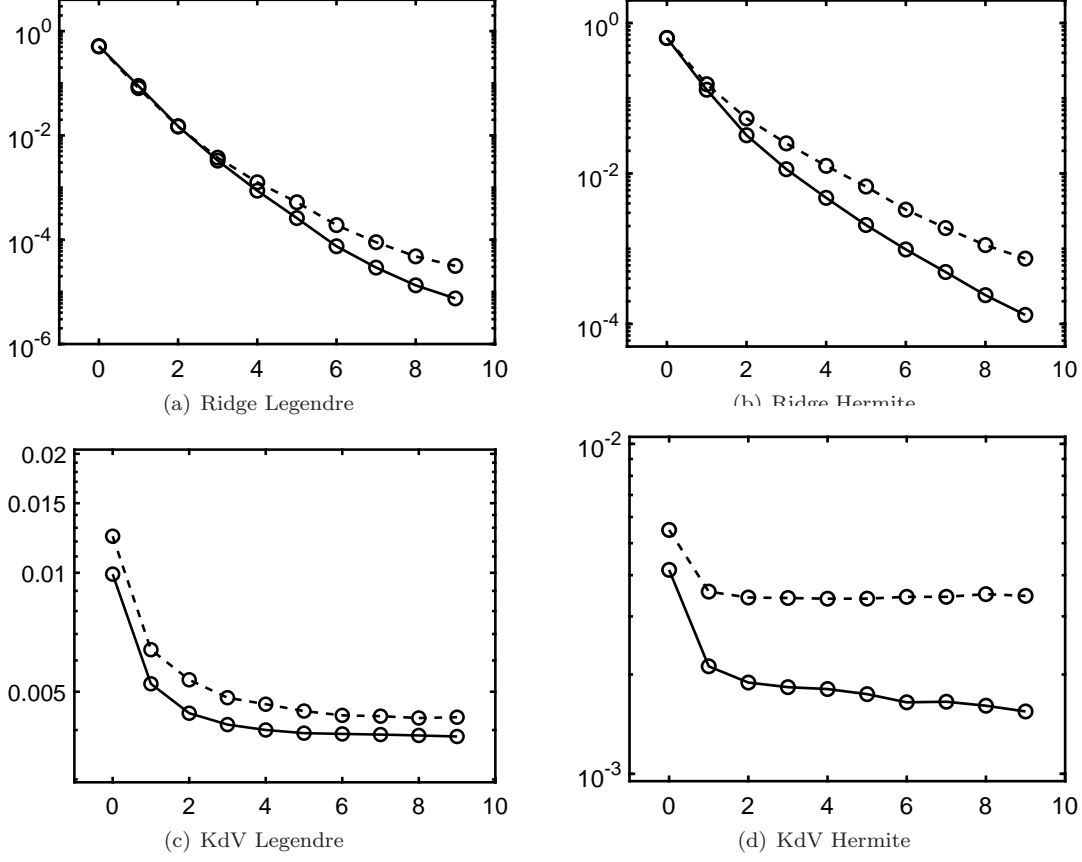


Figure 5: Relative error vs rotation. The size of Ψ is 160×455 in the Ridge problem and 160×1001 in the KdV problem.

the gPC expansions from a small amount of data. In particular, the rotation is determined by seeking the directions of maximum variation for the QoI through SVD of the gradients at different points in the parameter space. The linear system after rotations becomes ill-posed, specifically more coherent, which motivated us to choose the ℓ_1 - ℓ_2 method for sparse recovery. We conducted extensive simulations under various scenarios, including ridge function, KdV equation, and HD function with Legendre, Hermite, and Laguerre polynomials, all of which are widely used in practice. Our experimental results demonstrated the proposed combination of rotation and ℓ_1 - ℓ_2 significantly outperforms the standard ℓ_1 minimization (without rotation) and the rotational CS with the ℓ_1 approach.

Table 3: Computation time per each random realization, averaged over 20 trials. (N/A means a certain case is not available.)

Time (sec.)	dimension	rotations	Legendre	Hermite	Laguerre
Ridge function	160×455	9	6.53	4.31	16.19
KdV equation	160×1001	3	15.03	14.33	N/A
HD function	1000×5151	3	2041.82	2102.04	N/A

Acknowledgement

This work was partially supported by NSF CAREER 1846690. Xiu Yang was supported by the U.S. Department of Energy (DOE), Office of Science, Office of Advanced Scientific Computing Research (ASCR) as part of Multifaceted Mathematics for Rare, Extreme Events in Complex Energy and Environment Systems (MACSER).

References

- [1] B. ADCOCK, *Infinite-dimensional compressed sensing and function interpolation*, Found. of Comput. Math., (2017), pp. 1–41.
- [2] B. ADCOCK, S. BRUGIAPAGLIA, AND C. G. WEBSTER, *Compressed sensing approaches for polynomial approximation of high-dimensional functions*, in Compressed Sensing and its Applications, Springer, 2017, pp. 93–124.
- [3] N. ALEMAZKOOR AND H. MEIDANI, *Divide and conquer: An incremental sparsity promoting compressive sampling approach for polynomial chaos expansions*, Comput. Methods Appl. Mech. Eng., 318 (2017), pp. 937–956.
- [4] I. BABUŠKA, F. NOBILE, AND R. TEMPONE, *A stochastic collocation method for elliptic partial differential equations with random input data*, SIAM Rev., 52 (2010), pp. 317–355.
- [5] A. S. BANDEIRA, E. DOBRIBAN, D. G. MIXON, AND W. F. SAWIN, *Certifying the restricted isometry property is hard*, IEEE Trans. Inf. Theory, 59 (2013), pp. 3448–3450.
- [6] G. BLATMAN AND B. SUDRET, *Adaptive sparse polynomial chaos expansion based on least angle regression*, J. Comput. Phys., 230 (2011), pp. 2345–2367.
- [7] S. BOYD, N. PARIKH, E. CHU, B. PELEATO, AND J. ECKSTEIN, *Distributed optimization and statistical learning via the alternating direction method of multipliers*, Found. Trends Mach. Learn., 3 (2011), pp. 1–122.
- [8] A. M. BRUCKSTEIN, D. L. DONOHO, AND M. ELAD, *From sparse solutions of systems of equations to sparse modeling of signals and images*, SIAM Rev., 51 (2009), pp. 34–81.
- [9] R. H. CAMERON AND W. T. MARTIN, *The orthogonal development of non-linear functionals in series of fourier-hermite functionals*, Ann. Math., (1947), pp. 385–392.
- [10] E. J. CANDÈS, *The restricted isometry property and its implications for compressed sensing*, C.R. Math., 346 (2008), pp. 589–592.
- [11] E. J. CANDÈS, J. K. ROMBERG, AND T. TAO, *Stable signal recovery from incomplete and inaccurate measurements*, Comm. Pure Appl. Math, 59 (2006), pp. 1207–1223.
- [12] E. J. CANDÈS AND M. B. WAKIN, *An introduction to compressive sampling*, IEEE Signal Process. Mag., 25 (2008), pp. 21–30.
- [13] E. J. CANDÈS, M. B. WAKIN, AND S. P. BOYD, *Enhancing sparsity by reweighted l_1 minimization*, J. Fourier Anal. Appl., 14 (2008), pp. 877–905.
- [14] R. CHARTRAND, *Exact reconstruction of sparse signals via nonconvex minimization*, IEEE Signal Process Lett., 14 (2007), pp. 707–710.
- [15] P. G. CONSTANTINE, E. DOW, AND Q. WANG, *Active subspace methods in theory and practice: Applications to kriging surfaces*, SIAM J. Sci. Comput., 36 (2014), pp. A1500–A1524.

- [16] W. DAI AND O. MILENKOVIC, *Subspace pursuit for compressive sensing: Closing the gap between performance and complexity*, tech. rep., ILLINOIS UNIV AT URBANA-CHAMPAIGN, 2008.
- [17] D. L. DONOHO, *Compressed sensing*, IEEE Trans. Inf. Theory, 52 (2006), pp. 1289–1306.
- [18] D. L. DONOHO AND M. ELAD, *Optimally sparse representation in general (nonorthogonal) dictionaries via l_1 minimization*, Proc. Nat. Acad. Sci. USA, 100 (2003), pp. 2197–2202.
- [19] D. L. DONOHO, M. ELAD, AND V. N. TEMLYAKOV, *Stable recovery of sparse overcomplete representations in the presence of noise*, IEEE Trans. Inf. Theory, 52 (2006), pp. 6–18.
- [20] A. DOOSTAN AND H. OWHADI, *A non-adapted sparse approximation of PDEs with stochastic inputs*, J. Comput. Phys., 230 (2011), pp. 3015–3034.
- [21] O. G. ERNST, A. MUGLER, H.-J. STARKLOFF, AND E. ULLMANN, *On the convergence of generalized polynomial chaos expansions*, ESAIM: Math. Model. Numer. Anal., 46 (2012), pp. 317–339.
- [22] S. FOUCART AND H. RAUHUT, *A mathematical introduction to compressive sensing*, vol. 1, Birkhäuser Basel, 2013.
- [23] R. G. GHANEM AND P. D. SPANOS, *Stochastic finite elements: a spectral approach*, Springer-Verlag, New York, 1991.
- [24] R. GRIBONVAL AND M. NIELSEN, *Sparse representations in unions of bases*, IEEE Trans. Inf. Theory, 49 (2003), pp. 3320–3325.
- [25] W. GUO, Y. LOU, J. QIN, AND M. YAN, *A novel regularization based on the error function for sparse recovery*, arXiv preprint arXiv:2007.02784, (2020).
- [26] J. HAMPTON AND A. DOOSTAN, *Compressive sampling of polynomial chaos expansions: Convergence analysis and sampling strategies*, J. Comput. Phys., 280 (2015), pp. 363–386.
- [27] ———, *Basis adaptive sample efficient polynomial chaos (base-pc)*, J. Comput. Phys., 371 (2018), pp. 20–49.
- [28] J. D. JAKEMAN, M. S. ELDRED, AND K. SARGSYAN, *Enhancing ℓ_1 -minimization estimates of polynomial chaos expansions using basis selection*, J. Comput. Phys., 289 (2015), pp. 18–34.
- [29] J. D. JAKEMAN, A. NARAYAN, AND T. ZHOU, *A generalized sampling and preconditioning scheme for sparse approximation of polynomial chaos expansions*, SIAM J. Sci. Comput., 39 (2017), pp. A1114–A1144.
- [30] M. JARDAK, C.-H. SU, AND G. E. KARNIADAKIS, *Spectral polynomial chaos solutions of the stochastic advection equation*, J. Sci. Comput., 17 (2002), pp. 319–338.
- [31] M.-J. LAI, Y. XU, AND W. YIN, *Improved iteratively reweighted least squares for unconstrained smoothed ℓ_q minimization*, SIAM J. Numer. Anal., 51 (2013), pp. 927–957.
- [32] H. LEI, X. YANG, Z. LI, AND G. E. KARNIADAKIS, *Systematic parameter inference in stochastic mesoscopic modeling*, J. Comput. Phys., 330 (2017), pp. 571–593.
- [33] H. LEI, X. YANG, B. ZHENG, G. LIN, AND N. A. BAKER, *Constructing surrogate models of complex systems with enhanced sparsity: quantifying the influence of conformational uncertainty in biomolecular solvation*, SIAM Multiscale Model. Simul., 13 (2015), pp. 1327–1353.
- [34] K.-C. LI, *Sliced inverse regression for dimension reduction*, J. Am. Stat. Assoc., 86 (1991), pp. 316–327.
- [35] Y. LOU AND M. YAN, *Fast l_1 - l_2 minimization via a proximal operator*, J. Sci. Comput., 74 (2018), pp. 767–785.

- [36] Y. LOU, P. YIN, Q. HE, AND J. XIN, *Computing sparse representation in a highly coherent dictionary based on difference of L_1 and L_2* , J. Sci. Comput., 64 (2015), pp. 178–196.
- [37] Y. LOU, P. YIN, AND J. XIN, *Point source super-resolution via non-convex l_1 based methods*, J. Sci. Comput., 68 (2016), pp. 1082–1100.
- [38] J. LV, Y. FAN, ET AL., *A unified approach to model selection and sparse recovery using regularized least squares*, Annals of Stat., 37 (2009), pp. 3498–3528.
- [39] X. MA AND N. ZABARAS, *An adaptive high-dimensional stochastic model representation technique for the solution of stochastic partial differential equations*, J. Comput. Phys., 229 (2010), pp. 3884–3915.
- [40] C. MCDIARMID, *On the method of bounded differences*, Surveys in combinatorics, 141 (1989), pp. 148–188.
- [41] B. K. NATARAJAN, *Sparse approximate solutions to linear systems*, SIAM J. Comput., 24 (1995), pp. 227–234.
- [42] H. OGURA, *Orthogonal functionals of the Poisson process*, IEEE Trans. Inf. Theory, 18 (1972), pp. 473–481.
- [43] J. PENG, J. HAMPTON, AND A. DOOSTAN, *A weighted ℓ_1 -minimization approach for sparse polynomial chaos expansions*, J. Comput. Phys., 267 (2014), pp. 92–111.
- [44] ———, *On polynomial chaos expansion via gradient-enhanced ℓ_1 -minimization*, J. Comput. Phys., 310 (2016), pp. 440–458.
- [45] T. PHAM-DINH AND H. A. LE-THI, *A D.C. optimization algorithm for solving the trust-region sub-problem*, SIAM J. Optim., 8 (1998), pp. 476–505.
- [46] ———, *The DC (difference of convex functions) programming and DCA revisited with DC models of real world nonconvex optimization problems*, Annals Oper. Res., 133 (2005), pp. 23–46.
- [47] Y. RAHIMI, C. WANG, H. DONG, AND Y. LOU, *A scale invariant approach for sparse signal recovery*, SIAM J. Sci. Comput., 41 (2019), pp. A3649–A3672.
- [48] H. RAUHUT AND R. WARD, *Sparse legendre expansions via l_1 -minimization*, J. Approx. Theory, 164 (2012), pp. 517–533.
- [49] H. RAUHUT AND R. WARD, *Interpolation via weighted ℓ_1 minimization*, Appl. Comput. Harmon. Anal., 40 (2016), pp. 321 – 351.
- [50] T. M. RUSSI, *Uncertainty quantification with experimental data and complex system models*, PhD thesis, UC Berkeley, 2010.
- [51] K. SARGSYAN, C. SAFTA, H. N. NAJM, B. J. DEBUSSCHERE, D. RICCIUTO, AND P. THORNTON, *Dimensionality reduction for complex models via bayesian compressive sensing*, Int. J. Uncertain. Quantif., 4 (2014).
- [52] X. SHEN, W. PAN, AND Y. ZHU, *Likelihood-based selection and sharp parameter estimation*, J. Am. Stat. Assoc., 107 (2012), pp. 223–232.
- [53] S. SMOLYAK, *Quadrature and interpolation formulas for tensor products of certain classes of functions*, Sov. Math. Dokl., 4 (1963), pp. 240–243.
- [54] M. TAO AND Y. LOU, *Minimization of l_1 over l_2 for sparse signal recovery with convergence guarantee*. http://www.optimization-online.org/DB_HTML/2020/10/8064.html, Oct 2020.

- [55] M. A. TATANG, W. PAN, R. G. PRINN, AND G. J. MCRAE, *An efficient method for parametric uncertainty analysis of numerical geophysical models*, J. Geophys. Res-Atmos. (1984–2012), 102 (1997), pp. 21925–21932.
- [56] A. M. TILLMANN AND M. E. PFETSCH, *The computational complexity of the restricted isometry property, the nullspace property, and related concepts in compressed sensing*, IEEE Trans. Inf. Theory, 60 (2014), pp. 1248–1259.
- [57] R. TIPIREDDY AND R. GHANEM, *Basis adaptation in homogeneous chaos spaces*, J. Comput. Phys., 259 (2014), pp. 304–317.
- [58] P. TSILIFIS, X. HUAN, C. SAFTA, K. SARGSYAN, G. LACAZE, J. C. OEFELEIN, H. N. NAJM, AND R. G. GHANEM, *Compressive sensing adaptation for polynomial chaos expansions*, J. Comput. Phys., 380 (2019), pp. 29–47.
- [59] C. WANG, M. YAN, Y. RAHIMI, AND Y. LOU, *Accelerated schemes for the L_1/L_2 minimization*, IEEE Trans. Signal Process., 68 (2020), pp. 2660–2669.
- [60] D. XIU AND J. S. HESTHAVEN, *High-order collocation methods for differential equations with random inputs*, SIAM J. Sci. Comput., 27 (2005), pp. 1118–1139.
- [61] D. XIU AND G. E. KARNIADAKIS, *The Wiener-Askey polynomial chaos for stochastic differential equations*, SIAM J. Sci. Comput., 24 (2002), pp. 619–644.
- [62] Z. XU, X. CHANG, F. XU, AND H. ZHANG, *$L_{1/2}$ regularization: A thresholding representation theory and a fast solver*, IEEE Trans. Neural Netw. Learn. Syst., 23 (2012), pp. 1013–1027.
- [63] Z. XU AND T. ZHOU, *On sparse interpolation and the design of deterministic interpolation points*, SIAM J. Sci. Comput., 36 (2014), pp. A1752–A1769.
- [64] L. YAN, L. GUO, AND D. XIU, *Stochastic collocation algorithms using l_1 -minimization*, Int. J. Uncertain. Quan., 2 (2012), pp. 279–293.
- [65] L. YAN, Y. SHIN, AND D. XIU, *Sparse approximation using ℓ_1 - ℓ_2 minimization and its application to stochastic collocation*, SIAM J. Sci. Comput., 39 (2017), pp. A229–A254.
- [66] X. YANG, D. A. BARAJAS-SOLANO, W. S. ROSENTHAL, AND A. M. TARTAKOVSKY, *PDF estimation for power grid systems via sparse regression*, arXiv preprint arXiv:1708.08378, (2017).
- [67] X. YANG, M. CHOI, G. LIN, AND G. E. KARNIADAKIS, *Adaptive ANOVA decomposition of stochastic incompressible and compressible flows*, J. Comput. Phys., 231 (2012), pp. 1587–1614.
- [68] X. YANG AND G. E. KARNIADAKIS, *Reweighted ℓ_1 minimization method for stochastic elliptic differential equations*, J. Comput. Phys., 248 (2013), pp. 87–108.
- [69] X. YANG, H. LEI, N. BAKER, AND G. LIN, *Enhancing sparsity of Hermite polynomial expansions by iterative rotations*, J. Comput. Phys., 307 (2016), pp. 94–109.
- [70] X. YANG, H. LEI, P. GAO, D. G. THOMAS, D. L. MOBLEY, AND N. A. BAKER, *Atomic radius and charge parameter uncertainty in biomolecular solvation energy calculations*, J. Chem. Theory Comput., 14 (2018), pp. 759–767.
- [71] X. YANG, W. LI, AND A. TARTAKOVSKY, *Sliced-inverse-regression-aided rotated compressive sensing method for uncertainty quantification*, SIAM/ASA J. Uncertainty, 6 (2018), pp. 1532–1554.
- [72] X. YANG, X. WAN, L. LIN, AND H. LEI, *A general framework for enhancing sparsity of generalized polynomial chaos expansions*, Int. J. Uncertain. Quantif., 9 (2019).

- [73] P. YIN, E. ESSER, AND J. XIN, *Ratio and difference of l_1 and l_2 norms and sparse representation with coherent dictionaries*, Comm. Inf. Syst., 14 (2014), pp. 87–109.
- [74] P. YIN, Y. LOU, Q. HE, AND J. XIN, *Minimization of ℓ_{1-2} for compressed sensing*, SIAM J. Sci. Comput., 37 (2015), pp. A536–A563.
- [75] S. ZHANG AND J. XIN, *Minimization of transformed L_1 penalty: Closed form representation and iterative thresholding algorithms*, Comm. Math. Sci., 15 (2017), pp. 511–537.
- [76] ———, *Minimization of transformed L_1 penalty: theory, difference of convex function algorithm, and robust application in compressed sensing*, Math. Program., 169 (2018), pp. 307–336.
- [77] T. ZHANG, *Multi-stage convex relaxation for learning with sparse regularization*, in Adv. Neural Inf. Proces. Syst. (NIPS), 2009, pp. 1929–1936.
- [78] Z. ZHANG, X. YANG, I. V. OSELEDETS, G. E. KARNIADAKIS, AND L. DANIEL, *Enabling high-dimensional hierarchical uncertainty quantification by ANOVA and tensor-train decomposition*, IEEE Trans. Comput.-Aided Des. Integr. Circuits and Syst., 34 (2015), pp. 63–76.